

Supporting Information

Silva *et al.* 10.1073/pnas.0803626105

SI Methods

Fractionation of Native Human Plasma HDL. Albumin-free HDL3a ($d = 1.110\text{--}1.129$ g/ml) was isolated from normolipidemic human EDTA plasma by isopycnic density gradient ultracentrifugation as described in refs. 1 and 2.

Chemical Composition and Physical Property Characterization of rHDL.

The final phospholipid and protein compositions of the spherical and discoidal rHDL were determined by the analysis of phosphorus (3) and the Markwell modification of the Lowry protein assay (4), respectively. The free and total cholesterol contents of the spherical particles were determined enzymatically using a Roche Diagnostics kit (5). Cholesteryl ester concentrations were calculated as the difference between the total and free cholesterol concentrations. Triglyceride concentrations were determined enzymatically (6). Particle hydrodynamic diameters were measured by native polyacrylamide gradient gel electrophoresis (Phast System, Amersham Pharmacia) (7). Particle diameters were also calculated based on the negative stain electron microscopic measurements of the particles (see below).

Negative Stain Electron Microscopy. rHDL particles were negatively stained for electron microscopy by floating formvar-carbon-coated copper electron microscopy grids for 20 seconds on a 40 microliter droplet of particles in buffer. Excess fluid was removed from the grids. The grids, with adsorbed particles, were floated on a 40 microliter droplet of 1% phosphotungstic acid stain at pH 6.1 for 20 seconds. Excess stain was removed and the dried grids were viewed at 80 KeV with an FEI CM-12 transmission electron microscope. To determine the particle diameters, images were collected randomly from the sample. From each image, 5–10 particles were randomly selected for measurement. This process was continued until 200 particles had been measured for each condition. The diameters of discs within rouleaux were measured along the long axis of the particle. For individual oval or spherical particles, the diameter was taken as the longest visible axis. Particles having diameters of >2 standard deviations from the largest or smallest contiguous size classes were excluded from analysis as outliers. Such particles were rare and totaled $<1\%$ of particles measured. The microscope magnification was calibrated immediately before images were obtained.

Cryo-Electron Microscopy. HDL particles were diluted to 0.01 mg/ml using $1\times$ Delbecco's PBS (Invitrogen), 2.7 mM KCl, 1.46 mM KH_2PO_4 , 136.9 mM NaCl, and 8.1 mM Na_2HPO_4 . Samples (4 μl) were incubated for 1 min at room temperature, on Quantifoil holey carbon films coated 400 mesh copper grids (Quantifoil Micro Tools GmbH, Jena, Germany) rendered hydrophilic by glow-discharge for 20 seconds. The samples were flash-frozen and prepared as described in ref. 8. The frozen, hydrated particles embedded in vitreous ice over the holes in the carbon film were then transferred into liquid nitrogen for storage until used for Cryo-EM observation. HDL particles were examined at -183°C using the FEI (T12) Tecnai Spirit EM instrument operated at a 120 kV high tension, and the micrographs were acquired at three titled angles, -45° , 0° , and $+45^\circ$ under the low dose mode at a magnification of 67K by the GATAN 4,000 \times 4,000 high resolution CCD.

Circular Dichroism (CD). Both discoidal and spherical particle solutions were dialyzed against phosphate buffer (PB). Protein

concentration was determined using the modified Markwell-Lowry method and sample solutions were diluted to 100 $\mu\text{g}/\text{ml}$ with 20 mM PB. Concentrations were verified by A_{280} measurements after sample dilution. CD spectra of both discoidal and spherical rHDL particles were measured on a J-810 spectrometer (Jasco) using a 1 mm quartz CD cell (Starna). The measurements were an average of eight scans with a scan rate of 20 nm/min and a bandwidth of 0.2 nm with a time response of 2 s. Buffer spectra collected under the same conditions were subtracted to obtain the final spectra. The SELCON 3 method (a component of the CDPro software package) was used to estimate the fractional secondary structure of apoA-I in both particles.

Cross-Linking and Processing Samples for Mass Spectrometry. rHDL particles were cross-linked at 1 mg/ml apoA-I in PBS, at a molar ratio of protein to cross-linker of 1:10. The cross-linker used in these experiments was bis sulfo succinimidyl suberate (BS^3 , Pierce). Preparation and addition of the BS^3 stock solution to the protein was done within 1 min to minimize the competing aqueous hydrolysis reaction. The reaction was carried out for 24 h at 4°C with brief vortexing every 15 min for the first two hours. The reaction was quenched by addition of Tris-HCl to a final concentration of 100 mM. The proteins were then dialyzed against 10 mM ammonium bicarbonate buffer (pH 8.1) to remove small byproducts generated from cross-linking and hydrolysis reaction. After lyophilization followed by delipidation by standard techniques, the proteins were resuspended in 200 μl of standard Tris buffer (STB) containing 3M guanidine hydrochloride. Monomeric and dimeric cross-linked apoA-I species were separated from D79, S79, and D96 rHDL particles in the same buffer by gel filtration chromatography using the tandem gel filtration column set up (Superdex 200-Superose 6, 0.4 ml/min). Fractions corresponding to monomer and dimer as determined by coomassie-stained SDS/PAGE analysis were pooled separately and dialyzed against 10 mM ammonium bicarbonate buffer. S93 rHDL with three apoA-I per particle was processed without separating into its cross-linked components monomer, dimer and trimer due to limited resolution power of the gel filtration technique and the limited sample. The samples were concentrated by ultrafiltration (membrane MWCO 10,000, Millipore) to 1 mg/ml and digested with sequencing grade trypsin (Cat No. V5111, Promega) at 2.5% wt/wt enzyme/apoA-I at 37°C overnight. Next morning, 2.5% more trypsin was added for an additional 2 h. Aliquots (50 μg) of the digested protein samples were lyophilized and stored at -20°C until used for mass spectrometric analysis.

Mass Spectrometric Measurements. The mass spectrometer (QStar XL) used in the study was equipped with an electrospray ionizer and a quadrupole time-of-flight (Q-ToF) dual analyzer equipped with an on-line capillary high performance liquid chromatograph (HPLC, Agilent 1100). Tryptic peptides derived from the cross-linked rHDL samples were measured after optimization of the parameters and the gradient for human unmodified apoA-I tryptic peptide identification. Samples were resuspended in 0.1% trifluoroacetic acid in water (2 $\mu\text{g}/\mu\text{l}$). 30 pmols were injected into the HPLC and separated on a C18 capillary reversed phase column (Vydac, 500 $\mu\text{m} \times 15$ cm). The tryptic peptide elution was carried out by application of an acetonitrile gradient of 0–40% in 60 min at a flow rate of 6.0 $\mu\text{l}/\text{min}$, which was optimized for the separation of tryptic peptides from human apoA-I. The eluting peaks were subjected to subsequent mass

spectrometric detection in the range 300–1800 m/z . Automated MS/MS sequencing was carried out between 100 and 2000 m/z in Q2 pulsing mode. The mass spectrometer was set to acquire MS and MS/MS data in an automated fashion using the Information Dependent Acquisition (IDA) functionality built in the Analyst QS software. Each MS spectrum acquired in 1 sec was followed by acquisition of three MS/MS spectra at 3 sec each of the three most intense ions after satisfying the dynamic exclusion criteria. The dynamic exclusion criteria allowed for generating an exclusion list of peptide masses already fragmented for a period of 60 sec with a mass tolerance of 100 ppm for match of a peptide mass.

Mass Spectrometry Data Analysis. For each mass spectrum collected, a mass list was generated using the AnalystQS 1.1 software (Applied Biosystems). The completeness of the computer generated mass list was verified by manual peak selection across the entire mass spectrum for the first experiment. To identify unmodified peptides, peptides containing a hydrolyzed cross-linker, and intrapeptide cross-links, the mass list was analyzed using GPMW 4.0 (www.gpmaw.com). Potential cross-linked peptide pairs (interpeptide cross-links) were identified using a manually constructed spreadsheet containing the masses of each possible peptide pair plus the mass of the added cross-linker component that link the two masses. Datasets collected later into the project were analyzed by a program developed in our laboratory, CrossID, that can simultaneously identify all types of masses, unmodified, hydrolyzed, intrapeptide cross-links and interpeptide cross-links. This program was tested on all prior datasets analyzed using manual spread sheets and GPMW as explained above to confirm its compatibility. Once a given mass was identified as a putative cross-linked peptide pair, the identification was confirmed by manual evaluation of the MS/MS sequence evidence. The inclusion criteria for interpeptide cross-links were as follows: (i) The mass must have

appeared in at least 2 replicate experiments from independent particle preparations within 10 ppm of calculated mass. (ii) The corresponding MS/MS spectrum must exhibit at least 50% of the b and y series of theoretical fragment ions expected. (iii) If the amino acid residue Pro is present in one of the peptides involved in cross-linking, special attention was paid to the MS/MS fragment ions, which occur right before or after the Pro residue, which yields more intense fragment ions compared with other fragment ions. The interpeptide cross-links that appeared repeatedly in datasets were mapped using the mass within 10 ppm deviations and HPLC elution time. In intrapeptide cross-links, MS/MS evidence was typically limited because of the proximity of the cross-linker to both ends of the peptide. These were assigned if they were identified by mass within 10 ppm of the theoretical mass in at least 2 batches, with HPLC elution time correlations in the Total Ion Chromatogram (TIC) and with 50% of the theoretical fragment ions. All of the reported masses were manually checked to confirm that the computer selections were accurate.

Building the Trefoil Molecular Model. The trefoil model was constructed based on the double belt model (9), constructed from two molecules of human apoA-I (40–243). Using MOE (Molecular Operating Environment 2006.08, The Chemical Computing Group Inc., Canada), the double belt model was triplicated. Two of the models were rotated 120 and 240° respectively, around two bend points (K133 and Y236). All three models were split on the two bend points and then one of the other half models was deleted. The subsequences were merged to form three apoA-I molecules. The residues around the bending points were subjected to energy minimization to relieve any serious steric clashes. The .pdb file can be downloaded from the Protein Model Database (<http://mi.caspar.it/PMDB/main.php>) using the accession code PM0075240.

1. Chapman MJ, Goldstein S, Lagrange D, Laplaud PM (1981) A density gradient ultracentrifugal procedure for the isolation of the major lipoprotein classes from human serum. *J Lipid Res* 22:339–358.
2. Guerin M, et al. (2002) Dose-dependent action of atorvastatin in type IIB hyperlipidemia: Preferential and progressive reduction of atherogenic apoB-containing lipoprotein subclasses (VLDL-2, IDL, small dense LDL) and stimulation of cellular cholesterol efflux. *Atherosclerosis* 163:287–296.
3. Sokoloff L, Rothblat GH (1974) Sterol to phospholipid molar ratios of L cells with qualitative and quantitative variations of cellular sterol. *Proc Soc Exp Biol Med* 146:1166–1172.
4. Markwell MA, Haas SM, Bieber LL, Tolbert NE (1978) A modification of the Lowry procedure to simplify protein determination in membrane and lipoprotein samples. *Anal Biochem* 87:206–210.
5. Stahlner F, Gruber W, Stinshoff K, Roschlau P (1977) [A practical enzymatic cholesterol determination]. *Med Lab (Stuttg)* 30:29–37.
6. Wahlefeld AW (1974), ed Bergmeyer HU (Academic, New York), pp 1831–1835.
7. Davidson WS, et al. (1995) Effects of acceptor particle size on the efflux of cellular free cholesterol. *J Biol Chem* 270:17106–17113.
8. Ren G, Reddy VS, Cheng A, Melnyk P, Mitra AK (2001) Visualization of a water-selective pore by electron crystallography in vitreous ice. *Proc Natl Acad Sci USA* 98:1398–1403.
9. Segrest JP, et al. (1999) A detailed molecular belt model for apolipoprotein A-I in discoidal high density lipoprotein. *J Biol Chem* 274:31755–31758.
10. Silva RA, Hilliard GM, Li L, Segrest JP, Davidson WS (2005) A Mass Spectrometric Determination of the Conformation of Dimeric Apolipoprotein A-I in Discoidal High Density Lipoproteins. *Biochemistry* 44:8600–8607.
11. Davidson WS, Hilliard GM (2003) The spatial organization of apolipoprotein A-I on the edge of discoidal high density lipoprotein particles: A mass spectrometry study. *J Biol Chem* 278:27199–27207.
12. Wu Z, et al. (2007) The refined structure of nascent HDL reveals a key functional domain for particle maturation and dysfunction. *Nat Struct Mol Biol* 14:861–868.

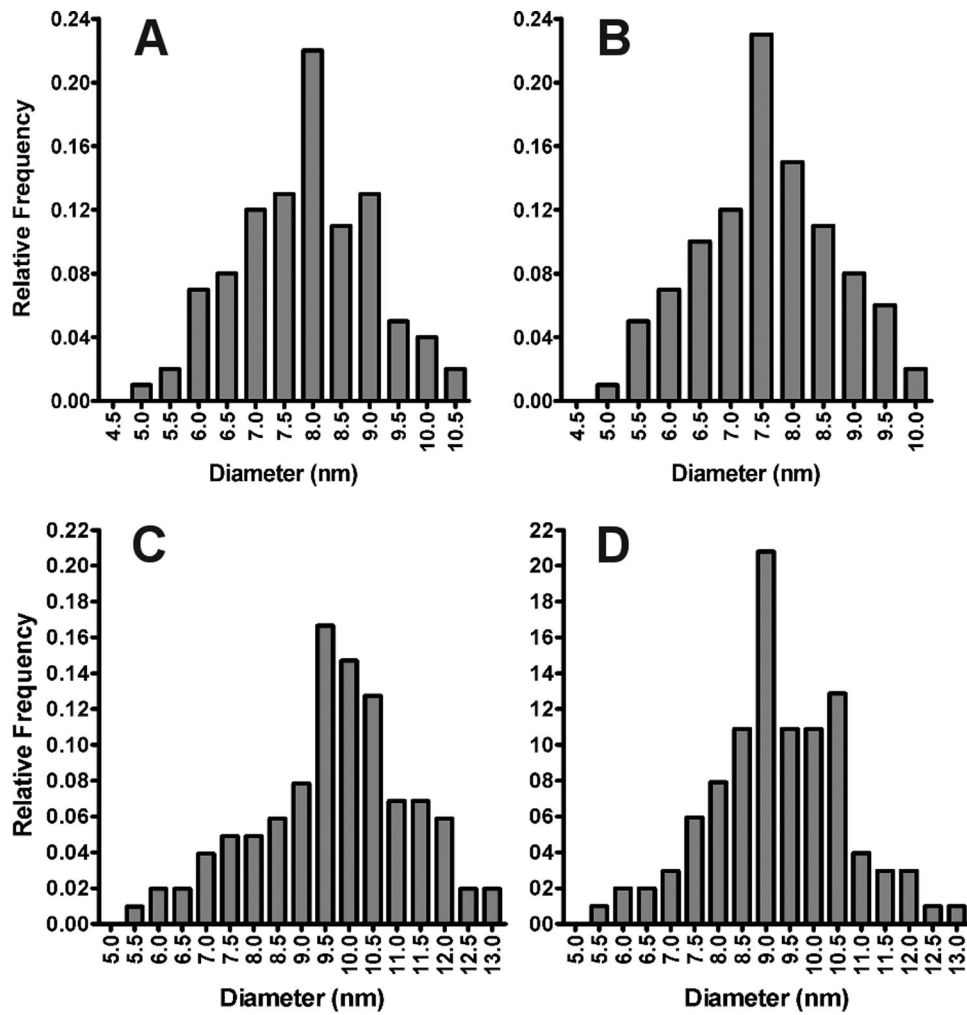


Fig. S1. Determination of particle diameters by image analysis of negative stain EM images. (A–D) Histograms determined from 200 randomly picked particle measurements per image from D79, S80, D96, and S93 samples respectively.

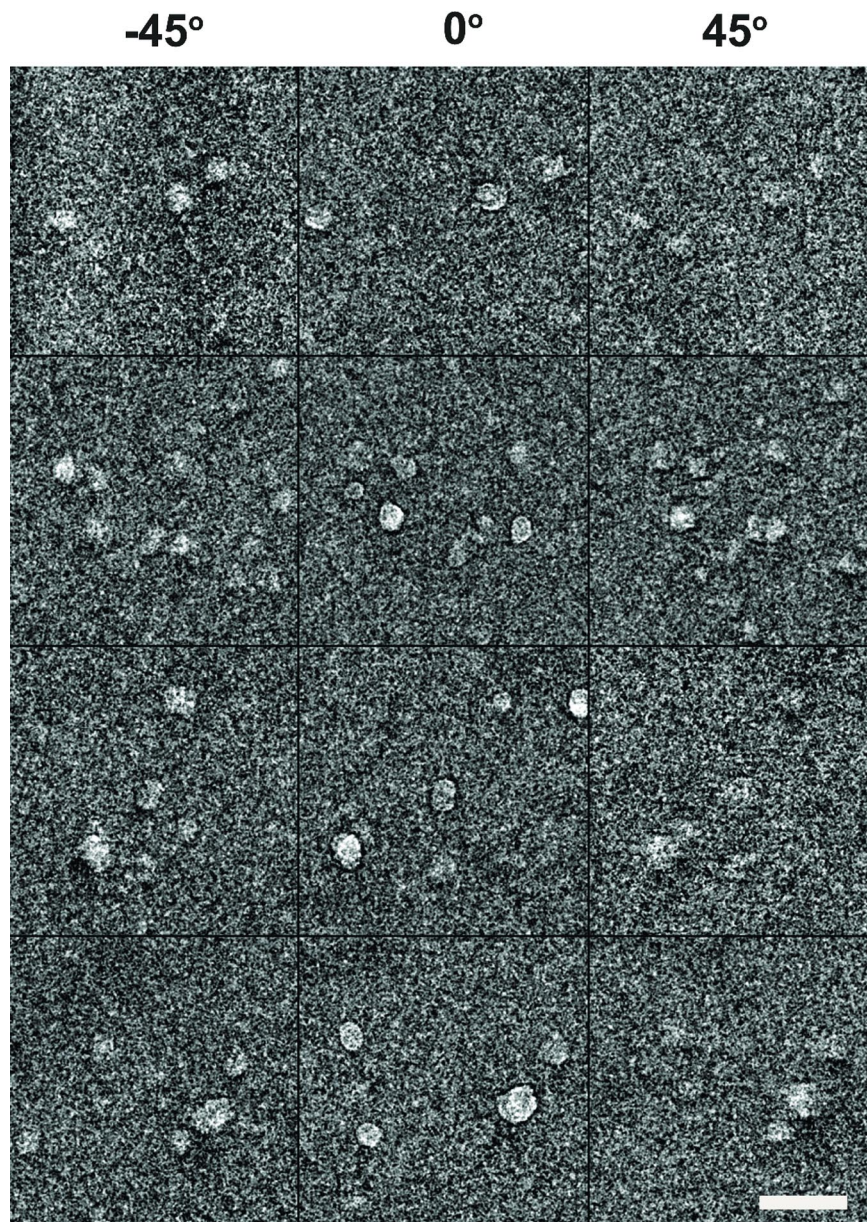


Fig. S2. Orthogonal tilt cryo-EM images of S93 particles. Images were collected at 3 different tilt angles: -45° (left lane), 0° (middle lane), and 45° (right lane). (Scale bar: 20 nm.)

Table S1. Intra and inter molecular cross-links identified in all HDL particles in this study

X-link	Peptide/Peptide		Theoretical mass, Da	Inter/intra*	D79	S80	D96	S93	HDL _{3a}	Possible Registry
K88-K94	84-96		1,671.8387	Intra	√	√	√	√	√	NA
K96-K106	95-107		1,716.9084	Intra	√	√	√	√	√	NA
K182-K239	178-188	239-243	1,897.0267	?	---	---	---	√	√	5/2
K12-K23	11-27		2,015.0936	Intra	√	√	√	√	√	NA
K238-K239	227-243		2,108.1039	Intra	√	√	√	√	√	NA
K118-K133	117-123	132-140	2,158.2108	Intra [†]	---	√	---	√	---	NA
K208-K208	207-215x	207-215	2,161.2104	Inter	√	√	√	√	√	5/2
N _T -K118	1-10	117-123	2,232.1172	?	---	---	---	√	√	--
N _T -K94	1-10x	89-96	2,294.1064	Intra	√	√	√	√	√	NA
K94-K96	89-106	---	2,302.1730	Intra	√	√	√	√	√	NA
K133-K140	132-149	---	2,302.1988	Intra	√	√	√	√	√	NA
K206-K208	196-215	---	2,346.2428	Intra	√	√	√	√	√	NA
K107-K118	107-116x	117-123	2,417.2411	Intra	√	---	√	---	---	NA
K96-K118	95-106x	117-123	2,457.3265	Inter	√	---	√	√	√	5/2
K12-K94	11-23	89-96	2,530.4143	Intra [†]	---	√	---	√	√	--
K23-K94	13-27	89-96	2,718.4325	Inter	√	√	---	---	---	--
K40-K239	28-45x	239-243	2,736.4332	Inter	√	√	√	√	√	5/5
N _T -K106	1-10	97-107	2,743.3127	intra [†]	---	√	---	√	√	--
K182-K238	178-188	227-239	2,808.4906	Inter	√	√	---	√	√	5/2
N _T -K12	1-10	11-23	2,825.4485	Intra [†]	---	√	---	√	√	NA
K226-K238	216-239	---	2,863.5620	Intra	√	√	---	---	---	NA
K118-K140	117-123x	134-149	2,914.5584	Inter	√	√	√	√	√	5/5
K88-K96	84-94x	95-106	2,923.4522	Intra	√	√	√	√	√	NA
K59-K208	46-61x	207-215	3,030.6023	Inter	√	√	√	√	√	5/5
K118-K133 or 118-140	117-123	132-149	3,326.7902	Intra	√	---	---	---	---	NA
K226-K239	216-238x	239-243	3,337.8059	Inter	---	---	√	---	---	NA
K226-K239	216-238x	239-243	3,337.8059	Intra	√	---	---	---	---	NA
K40-K238	28-45	227-239	3,647.8972	Inter	√	---	---	---	---	5/5
K40-K45	28-59	---	3,727.8618	Intra	√	√	√	√	---	NA
K59-K195	46-61x	189-206	4,046.0634	Inter	---	---	√	---	---	5/5
K77-K195	62-83	189-206	4,782.3662	Inter	√	√	√	√	√	5/5

*For most of the cross-links, intra- and intermolecular assignments were made based on D96 and D79 monomer and dimer separations (10).

[†]Cross-links that were assigned based on data from S80.

The two cross links indicated as "?" only appeared in the S93 sample. Inherent limitations of the method preclude a determination of the intra or intermolecular nature of these two cross-links. The method used to determine whether a cross-linker was "inter-molecular" or "intramolecular" was reported before (10,11). The intermolecular cross-links allow determination of the molecular registry and near neighbor interactions among apoA-I molecules incorporated on HDL particles. The intermolecular cross-links that we interpret to fit with the LL5/5 molecular registry are highlighted in blue whereas intermolecular cross-links we believe match with LL5/2 molecular registry are highlighted in yellow.

Many of the intramolecular cross-links were short range and therefore do not speak to registry of the molecules. These are indicated as NA (not applicable) in the registry column. Four long range intramolecular cross-links appeared in the spheres of both sizes (highlighted in gray) and may indicate flopping of the N terminus (1-43) of apoA-I in rHDL freely in the solution with its ability to cross-link with many residues. This was speculated by Wu et al based on hydrogen deuterium exchange experiments on rHDL particles (12).